DEVELOPMENT AND VALIDATION OF PHYSICS BASED MODELS FOR ICE SHEDDING

Avani Gupta, Elizabeth Halloran, and Lakshmi N. Sankar
agupta354@gatech.edu, ehalloran3@gatech.edu, lsankar@ae.gatech.edu
School of Aerospace Engineering
Georgia Institute of Technology, Atlanta, GA 30332-0150 (USA)

Jose Palacios
jlp324@engr.psu.edu
Department of Aerospace Engineering
The Pennsylvania State University, University Park, PA 16802 (USA)

Richard E. Kreeger
richard.e.kreeger@nasa.gov
NASA Glenn Research Center
Cleveland, OH 44135 (USA)

Abstract

Calculations for ice accretion and shedding are presented for a model scale rotor in hover. The aerodynamic characteristics of the rotor are first computed using a combined blade element-momentum theory. The effective angles of attack, and the local flow velocity are used within the NASA Glenn solver LEWICE to estimate the collection efficiency. The computed collection efficiency and the surface pressure distribution from a panel method within LEWICE are used to estimate the ice accretion over the rotor blades for a selected time interval. Finally, a force balance approach is used to establish shedding events where the centrifugal force over the ice mass exceeds the adhesive forces at the rotor surface and the cohesive forces between adjacent masses of ice. Preliminary comparisons with test data acquired at the Pennsylvania State Icing Research Tunnel are presented. Sensitivity of the ice shedding events to surface roughness, adhesive strength, cohesive strength, and ambient conditions is discussed.

1. INTRODUCTION

1.1. Motivation

Modern helicopters, civilian and military alike, are expected to operate in all weather conditions. Ice accretion adversely affects the availability, affordability, safety and survivability. Availability of the vehicle may be compromised if the ice formation requires excessive torque to operate the rotor with increasing drag. Due to weight and power requirements of currently certified electro-thermal ice protection systems, affordability of such protection is not always possible. Instrumenting the rotor blades with built-in heaters increases the cost of the helicopter, places further demands on the engine due to power consumption, and increases maintenance requirements. For unprotected vehicles, ice shedding events exceeding the imbalance carrying capability of the rotor could occur. Such events, combined with unexpected stall phenomena attributable to ice formation could severely affect the safety of the flight.

Given the importance of understanding the effects of icing on rotorcraft performance, considerable work has been done on the development of analytical and empirical tools, accompanied by wind tunnel and flight test data for model verification.

1.2. Related Experimental Studies

Potapczuk et al. give an excellent survey of the computational and experimental studies conducted in the field of aircraft icing prior to 1991 [1]. Before the advent of high speed computers, icing research for helicopters was focused on wind tunnel and flight tests. In 1981 and 1983, icing and deicing tests have been conducted with a model rotor of the Eurocopter Super Puma in the SIMA wind tunnel at France [2]. The influence of different parameters such as water droplet size, static temperature and liquid water content were investigated. It was found that speed and temperature significantly affect ice shape. Flight tests in icing condition were performed on a UH-1H helicopter in level flight during 1983-84 as part of the joint NASA / Army HIFT (Helicopter Icing Flight Test) program [3]. Considerably different ice shapes from those of the hover case were observed. The reason for this was explained by the unsteadiness of the flow field. In 1988, the first model rotor icing tests have been done with an OH-58 Tail Rotor Rig in the NASA Lewis Research Center Icing Research Tunnel (IRT) [4]. These studies established the usefulness of the Icing Research Tunnel as a facility for obtaining meaningful data for rotating systems. Subsequently, several wind tunnel tests have been conducted with a heavily instrumented subscale model of a generic helicopter main rotor by NASA at the IRT [5-9]. The effects of temperature, liquid water content (LWC), median droplet diameter, advance ratio, shaft angle, tip Mach number (rotor speed) and thrust coefficient were investigated.

More recently shedding events from rotor blades have been experimentally investigated by multiple authors. From 2006 to 2008, the Anti-icing Material International Laboratory (AMIL) in Canada performed sub-scale model rotor icing tests in collaboration with Bell Helicopter Textron to study ice physics, low energy de-icing systems and hydro- or ice-phobic coatings use for small helicopters [10]. Fortin [10] also proposed an analysis procedure for ice shedding and showed good correlation between prediction and experiment.

Beginning in 2009, over the past decade, model rotor icing tests in hover have been conducted by the Pennsylvania State University [11]. Prediction of ice shapes and shedding has been conducted at the institution. These authors used an approach similar to that of Fortin for shedding analysis. Extensive icing data for a two bladed tail rotor tested at the NASA Glenn Research Center have been reported by Kreeger [12] and Wright [13]. Available data include performance with and without icing, measured ice shapes, deicing, and shedding.

1.3. Prior Computational Studies

Several ice accretion tools have been developed internationally to predict ice shapes on airfoils, wings, inlets, rotors, and propellers for various operating conditions. Some of representative ice accretion programs are LEWICE [14], ONERA [15 - 17], FENSAP-ICE [18], and CANICE [19, 20]. Most of icing codes are primarily two-dimensional in nature, although some have been expanded into three dimensions, such as LEWICE 3D, FENSAP-ICE and ONERA 3D. Ice accretion programs may use a 2D or quasi-3D potential flow solver to obtain flow field or use a high fidelity analysis such as a Navier-Stokes solver to capture detailed viscous and unsteady effects. To determine the amount of water captured on surface, either a Lagrangian or an Eulerian approach could be used.

For the thermodynamic analysis of ice accretion processes, most ice accretion codes are based on the classical Messinger model [21].

Given the complexity of ice accretion and the cost of modelling aerodynamic performance for complex structures such as rotor blades, research has been conducted to develop empirical equation relating icing conditions to lift and drag degradation. Flemming [22] performed a series of tests with rotorcraft airfoils and formulated 2D airfoil section icing relationships for ice thickness and for changes in aerodynamic force and moment coefficients. The 2D empirical relationships have often been incorporated into rotorcraft comprehensive performance prediction codes. Britton [23, 24] developed an analytical approach calculating the performance degradation of a helicopter operating in an icing condition. Instead of using the empirical relationship developed by Flemming [22], an Interactive Boundary Layer method [25] was used to calculate the aerodynamic coefficients of iced geometries. Ice shape at each radial location was obtained by LEWICE. Zanazzi [26] conducted ice accretion simulations and reported rotor performance predictions in hover using CFD tools. For the prediction of ice growth, 2D analysis at each radial section based on classical Lagrangian approach and the Messinger model was performed. Heat transfer coefficients are obtained by using an integral boundary layer calculation method. Good correlation with experimental ice shapes was obtained at blade inboard regions (rime ice). There was a deviation between predictions and experimental data at the outboard sections (glaze ice). Glaze ice shapes are more difficult to predict since water does not freeze instantaneously and the heat transfer modelling equations are based on limited wind tunnel test data or other unverified modeling approaches. Bain [27-30], and Narducci [31, 32] also used a similar approach to that of Zanazzi [26] for modeling the ice accretion phenomena. Finally, Kim [33] has used a 3-D CFD analysis, coupled with an Eulerian droplet convection model patterned after Ref. 18, and an extended Messinger model to predict ice accretion and shedding for the two bladed rotor described in Ref. 12 and 13.

2. CURRENT PREDICTION APPROACH

The computational methodologies that may be employed to model rotorcraft icing are illustrated in Figure 1. The flight conditions pertaining to the specific case being simulated are first prescribed. The user has the option to use one of three options to model the external aerodynamics of the clean rotor configuration. The first is a low computational cost Blade Element Momentum (BEM) calculation with a prescribed or free wake model from which the effective angle of attack of the blade sections is extracted at every radial position of the blade. Alternatively, CFD solvers which yield a complete flow solution in a PLOT3D format may be used. GT-Hybrid is an in-house solver that couples the Navier-Stokes methodology to model the viscous flow over the blade with a Lagrangian wake representation to model the effects of the wake. In addition, the user can select to model the blade aerodynamics using OVERFLOW, which is NASA's overset structured grid CFD solver.

Once results from the clean configuration are obtained, ice accretion may be computed using one of two approaches. The first option is to use LEWICE, which is an industry standard program and has been developed under the direction of NASA Glenn Research Center. Alternatively, GT DROP and GT ICE, independent solvers developed by the present investigators at Georgia Tech to model the droplet impingement efficiency and the ice accretion, may be used. Both of these approaches output the new iced airfoil coordinates at different input radial stations along the blade. These coordinates are used to generate an iced surface of the blade, which is then used as an input for the shedding analysis.

Because the objective of the present studies was to assess the effects of physical factors on ice shedding phenomena, the BEM numerical approach was used to compute the flow conditions over the span of the blade. The approach adopted is highlighted in green in Figure 1. LEWICE was used for the computation of the ice shapes.

An empirical model to predict self-shedding was used. The procedure used to determine the length of the shed ice and the time at which shedding occurs is described below:

a. At any specified instant in time, the contact area, volume, and mass of the ice are computed.

b. The interface transverse shear stress at the blade surface between the ice shape and the blade and the cohesive stresses exerted on a segment of ice by the neighboring ice mass are computed. The cohesive stresses are based on the works of Fortin [10]. The surface shear stresses are based on temperature and on the rotor blade surface, using relationships derived from experimental data. In the present study, the following curve fit extracted from the data reported in Ref. 34 was used. The tests in Ref. 34 were performed on rotor blades made of Stainless Steel 430.

$$\text{Adhesive Strength (kPa)} = -14.358\,T - 62.652$$

Here the temperature T is expressed in degrees Celsius.

It should be noted that the adhesion strength is highly sensitive to material surface roughness. This particular curve fit does not consider those effects.

c. The components of the centrifugal, shear, and cohesive force vectors are computed, starting from the tip to the root, on sections on the rotor blade.

d. The feasibility of shedding is examined. It is assumed that all the ice mass outboard of a given radial location will be shed if the sum of applied forces (centrifugal, and optionally aerodynamic pressure) on the mass of ice exceeds the adhesion force at the surface and cohesion force between adjacent radial sections of ice.

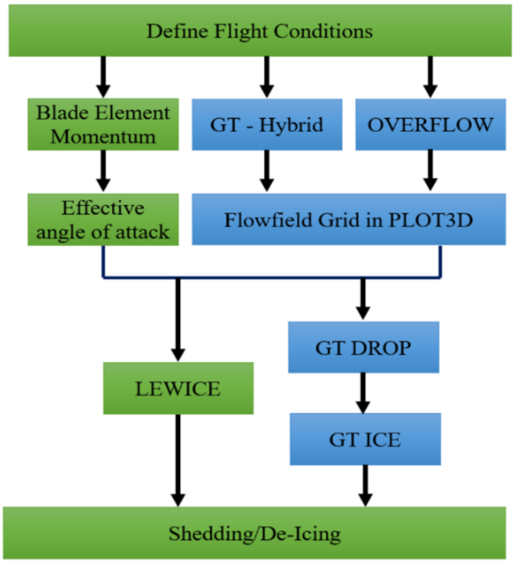

Figure 1. Methodologies for Modeling Rotor Ice Accretion and Shedding

3. TESTING FACILITY

The present studies made use of the shedding data collected at the Adverse Environment Rotor Test Stand (AERTS) facility at the Pennsylvania State University [11]. This is an industrial 6.1 × 6.1 × 3.6 m^3 cold chamber where temperatures between −25 °C and 0 °C can be achieved. In the middle of the ice chamber, an 89.5 kW motor powers the rotor. A maximum 1500 RPM with 1.37 m radius blades can be achieved reproducing full-scale helicopter tip speeds. Rotor performances are measured by a load cell, accelerometers and shaft torque sensor. Fifteen NASA standard icing nozzles are located in the chamber ceiling to generate the icing cloud. The nozzles inject atomized water droplets of controllable MVD inside the chamber.

The flow conditions for which ice accretion and shedding data available were available for this study are shown in Figure 2. The rotor tip speeds for the tests were limited to 600 RPM [11] for the validation cases and 450 RPM [35] for the sensitivity test cases.

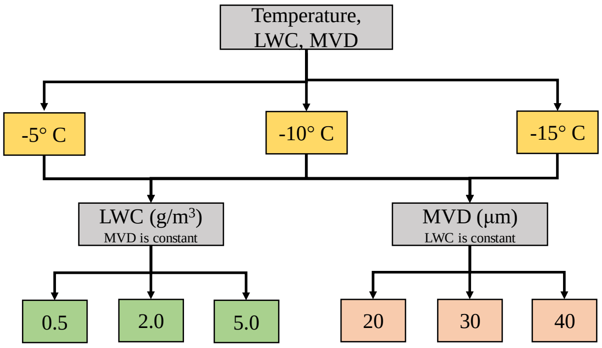

Parameter		Value
Rotor Diameter	Validation Cases	2.36 m
	Sensitivity Test Cases	2.86 m
Chord		0.172 m
Section		NACA 0015
Linear Twist (°)		-2.13
Collective Pitch (°)		2.5
Root Clearance		20 %

Figure 2. Test Data used in the Present Shedding Analyses

4. RESULTS AND DISCUSSION

As a starting point, ice shapes over the rotor, reported in Ref. 11, were computed. Figure 3 shows the computed and predicted ice shapes at two radial locations. The agreement is satisfactory, given the low computational cost aerodynamic model (combined blade element-momentum theory). The error in the ice thickness, calculated at the airfoil tip, is around -0.02 % for the case in Figure 3a. For the case in Figure 3b, it is higher at 13.0 %.

Table 1 presents a representative case with measured and the predicted, shedding locations. The predicted shedding location is within 3% R of the experimentally reported shedding location.

The effect of ambient temperature on ice growth was next examined. Figure 4 shows the computed ice shapes at several radial locations.

As expected, it is predicted that at lower temperatures, much of the ice formation occurs right near the nose of the airfoil, whereas significant runback of the water occurs at higher temperatures before it freezes (Figure 4). It is also seen that the higher flow velocities at the tip region gives rise to increased heat transfer and freezing, giving rise to horn shaped ice. It is known that as velocity, temperature, LWC or MVD increase, a transition from rime to glaze occurs.

It is also known based on the work of Soltis et al. [34] that the colder temperatures increased the adhesion strength at the surface. As a result, shedding was observed only for the warmest temperature of -5 degree C at 65% Radius.

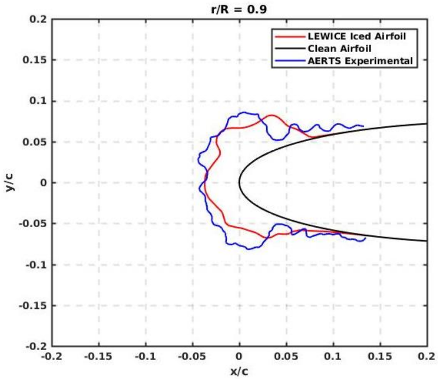

Ambient Temperature (°C)	-10.7
MVD (µm)	25
LWC (g/m³)	2.0
RPM	500
Collective Pitch (°)	2.5
Total Icing Time (s)	180

Figure 3a. Computed and Measured Ice Shape at 90% R, 500 RPM.

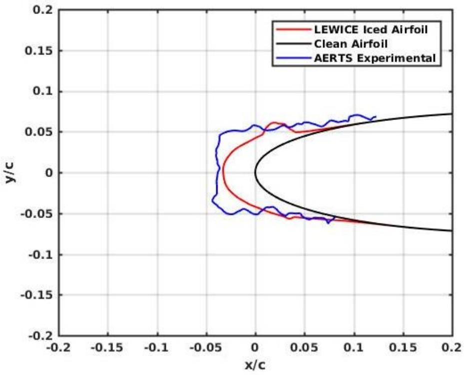

Ambient Temperature (°C)	-10.5
MVD (µm)	25
LWC (g/m³)	1.6
RPM	600
Collective Pitch (°)	2.5
Total Icing Time (s)	180

Figure 3b. Computed and Measured Ice Shape at 80% R, 600 RPM

Table 1: Experimental and Predicted Shedding Location at 600 RPM.

Parameter	Value
Temperature (° C)	-4.7
MVD (μm)	20
LWD (g/m^3)	6.9
RPM	600
Collective	2.5
Total Icing Time (s)	352
Exp. Shedding Location	77% R
Predicted Shedding Location	80% R

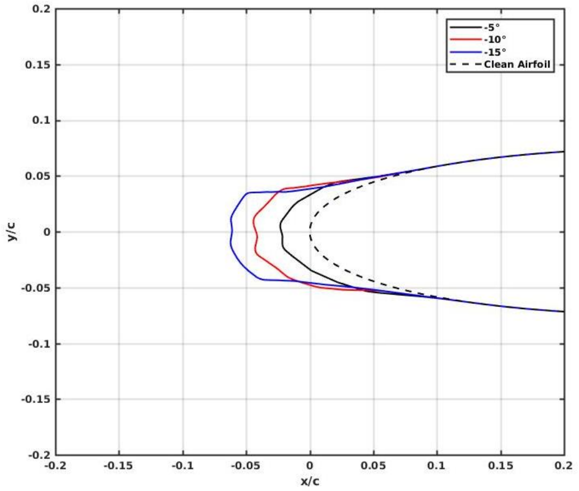

Figure 4a. 40%R

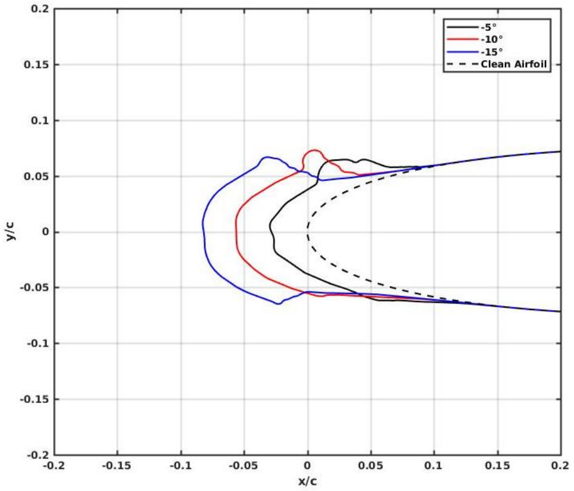

Figure 4b. 70%R

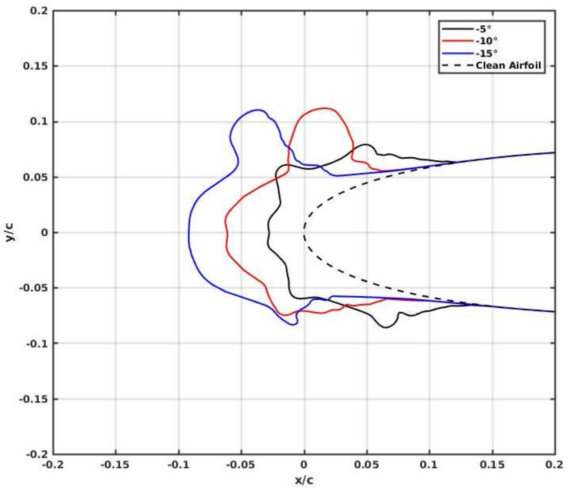

Figure 4c. 90% R

Figure 4. Effect of ambient temperature on ice shape (with LWC and MVD held fixed)

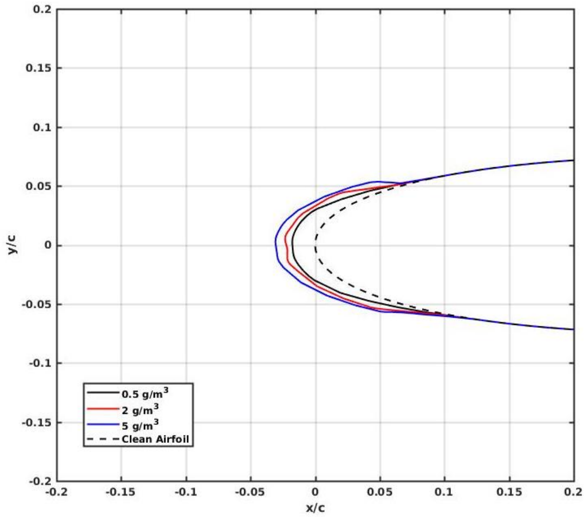

Figure 5a. 40%R

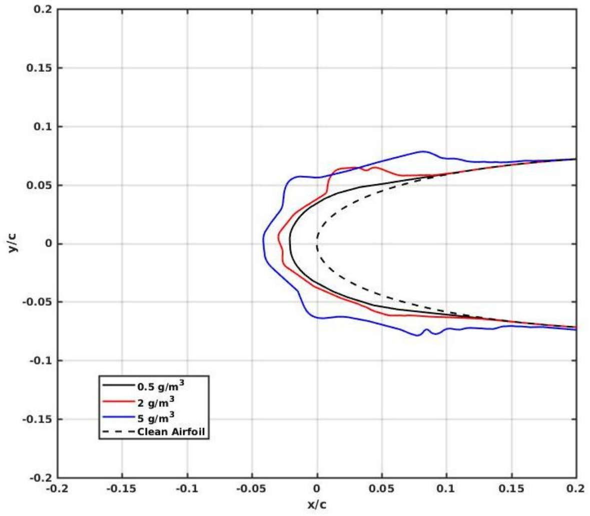

Figure 5b. 70% R

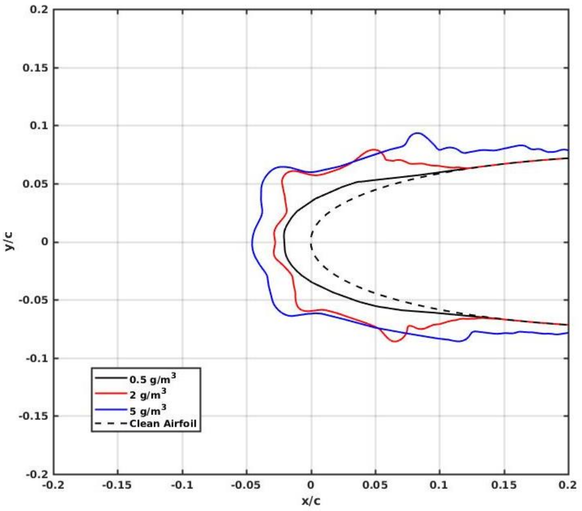

Figure 5c. 90%R

Figure 5. Effect of Liquid Water Content on Ice Shape

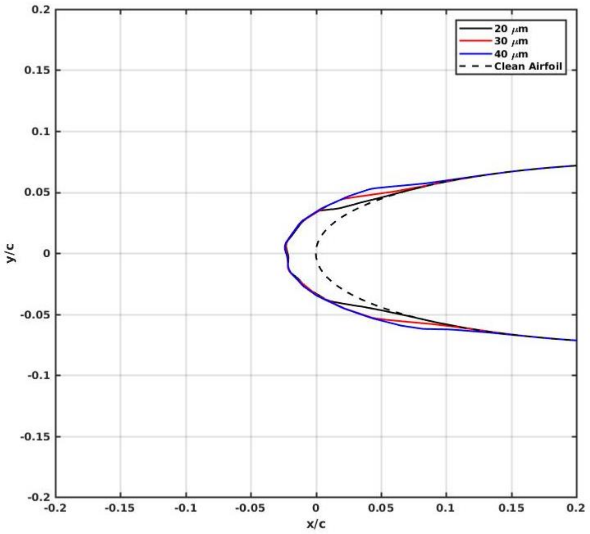

Figure 6a. 40% R

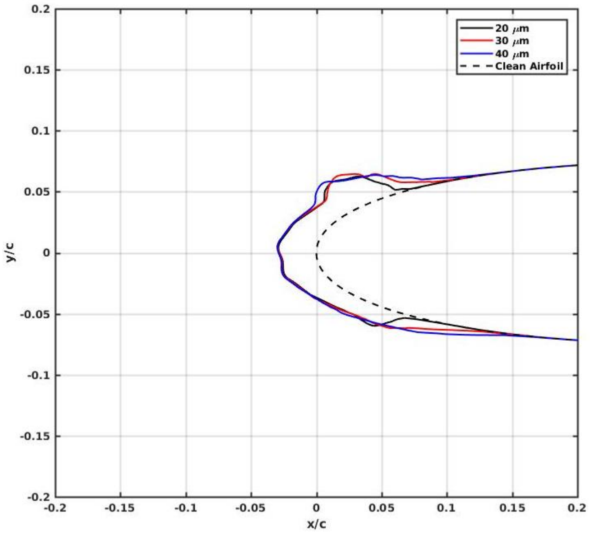

Figure 6b. 70%R

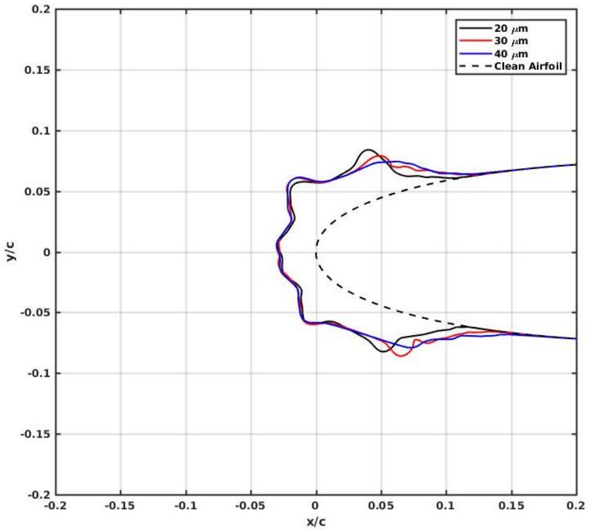

Figure 6c. 90% R

Figure 6. Effect of Droplet Diameter on Ice Shape

The effects of liquid water content on predicted ice shapes was next conducted, holding water droplet diameter and ambient temperature fixed. The liquid water content has a direct role on the mass of water deposited on the blade surface, and hence the mass of the ice that is accreted, as seen in figures 5. The excess water also runs back before freezing. Thus, while the mass of ice increases, so does the contact area of the ice at the surface, giving increased adhesion forces.

Finally, the effect of the water droplet diameter (MVD) on ice formation and shedding was done. Shown in Figure 6 are the computed ice shapes at three different radial locations. It is seen that the droplet diameter had a negligible effect on the computed ice shape.

Table A.1 in Appendix A summarizes all the cases that have been conducted, for multiple combinations of ambient temperature values, LWC, and liquid droplet diameter. Shedding was predicted for the warmest temperatures of -5 degrees Celsius, because of the lower adhesive stress values. At all other temperatures, shedding was not observed in our simulations and in the experimental studies.

5. CONCLUSIONS

The phenomenon of ice shedding has been systematically studied for model rotors in hover. A simple aerodynamic model based on the blade element momentum theory, and a 2-D ice accretion solver LEWICE applied in strip theory fashion, was used. In spite of its simplicity, this approach gives useful insight into the effects of physical factors such as ambient temperature, water droplet diameter, and liquid water content on computed ice shape and its variation along the surface. Shedding was predicted only for the warmest temperatures of -5 degrees Celsius, for large liquid water content. Droplet diameter played a negligible role on the computed ice shapes. Comparisons for ice shapes and shedding data from the AERTS facility was satisfactory, indicating that the proposed low-computational cost approach may be used as a first order tool for predicting shedding, at least for the low tip speed conditions testes to date.

Copyright Statement

References

[1] Potapczuk, M. G., and Reinmann, J. J., “Icing Simulation: A Survey of Computer Models and Experimental Facilities,” AGARD, Effects of Adverse Weather on Aerodynamics, 1991.

[2] Guffond D. P., "Icing and Deicing Test on a ¼ Scale Rotor in the ONERA SIMA Wind Tunnel," AIAA 24th Aerospace Science Meeting, January 6-9, Reno, Nevada, 1986.

[3] Lee, John D., Harding, Rorry and Palko, Richard L. “Documentation of Ice Shapes on the Main Rotor of a UH-1H Helicopter in Hover”. NASA CR 168332, 1984.

[4] Miller T. L. and Bond T. H., "Icing Research Tunnel Test of a Model Helicopter Rotor," NASA/TM-101978, 1989.

[5] Bond T. H., Flemming R. J. and Britton R. K., "Icing Tests of a Model Main Rotor,” AMS, Annual Forum 46th Washington, DC, USA, 1990.

[6] Flemming R., Britton R. K. and Bond T. H, "Model Rotor Icing Test in the NASA Lewis Icing Research Tunnel," NASA/TM-104351, 1991.

[7] Korkan K., "Experimental Study of Performance Degradation of a Rotating System in the NASA Lewis RC Icing Tunnel," NASA/CR-190684, 1991.

[8] Flemming R., Bond T. H. and Britton R. K., "Results of a Sub-Scale Model Rotor Icing Test," NASA/TM-103709, 1991.

[9] Britton R. K. and Bond T. H., "A Review of Ice Accretion Data from a Model Rotor Icing Test and Comparison with Theory," NASA/TM-103712 and AIAA-91-0661, 1991.

[10] Fortin, G. and Perron, J., “Spinning Rotor Blade Tests in Icing Wind Tunnel” Paper AIAA 2009-4260, 1st AIAA Atmospheric and Space Environments Conference, San Antonio, TX, 2009.

[11] E. W. Brouwers, J. L. Palacios, E. C. Smith, A. A. Peterson, "The experimental investigation of a rotor hover icing model with shedding," AHS 66th Annual Forum and Technology Display, Phoenix, USA, 2010.

[12] Kreeger, R. E. And Tsao, J., “Ice Shapes on a Tail rotor,” AIAA Paper 2014-2612, 6th AIAA Atmospheric and Space Environments Conference, Atlanta, GA, June 2014.

[13] Wright, J., Aubert, R., “Icing Wind Tunnel Test of a Full Scale Heated Tail Rotor Model,” American Helicopter Society 71st Annual Forum, Virginia Beach, Virginia, May 5–7, 2015.

[14] Wright, W. B., “User Manual for LEWICE Ver. 3.2,” NASA CR 214255, Cleveland, OH, 2008.

[15] Guffond, D.; Brunet L., "Validation du programme bidimensionnel de capitation," Chátillon Cedex, France: Office National D’Études et de Recherches Aérospatiales, 1988.

[16] Henry, R. "Development of an electrothermal de-icing/anti-icing model," Chatillon Cedex: Office National d’Etudes et de Recherches Aérospatiales, 1992.

[17] Montreuil, E., Chazottes, A., Guffond, D., Murrone, A., Caminade, F., and Catris, S. "Enhancement of Prediction Capability in Icing Accretion and related Performance Penalties Part I: Three-dimensional CFD Prediction of the Ice Accretion," Paper AIAA 2009-3969, 1st AIAA Atmospheric and Space Environments Conference, San Antonio, Texas, 2009.

[18] Beaugendre, H., Morency, F., and Habashi, W., “FENSAP-ICE’s Three-dimensional In-

Flight Ice Accretion Module: ICE3D," Journal of Aircraft, Vol. 40 No.2, 2003.

[19] Morency, F., Tezok, F., Paraschivoiu, I. "Anti-icing System Simulation using CANICE," Journal of Aircraft, v. 36, n. 6, 1999.

[20] Gouttebroze, S., Saeed, F., and Paraschivoiu, I., "CANICE- Capabilities and Current Status," in NATAO/RTO Workshop, Assessment of icing code prediction capabilities, CIRA, Capua, Italy, December 2000.

[21] Messinger, B. L., "Equilibrium temperature on an unheated icing surface as a function of airspeed," J. Aeronautical Sci. Vol. 20, 1953, pp. 29-41.

[22] Flemming, Robert J. and Lednicer, David A. "High Speed Ice Accretion on Rotorcraft Airfoils," NASA CR 3910 1985.

[23] Britton, Randall K, "Ongoing Development of a Computer Jobstream to Predict Helicopter Main Rotor Performance in Icing Condition," NASA CR 187076, 1991.

[24] Britton, Randall K, "Development of an Analytical Method to Predict Helicopter Main Rotor Performance in Icing Condition," NASA CR 189110, 1992.

[25] Cebeci, T., "Calculation of Flow Over Iced Airfoils," AIAA Journal, Vol. 27, 1989, pp. 853-861.

[26] G.Zanazzi, G.Mingione, A. Pagano, A. Visingardi, "Ice Accretion Prediction on Helicopter Rotor Blade in Hover Flight," SAE Aircraft and Engine Icing International Conference, SAE Paper 2007-01-3309, 2007.

[27] Bain, J., Sankar, L. N., Nucci, M., Egolf, A., and Flemming, R. J., "A Methodology for Modeling the Effects of Icing on Rotary Wing Aerodynamics," Proceedings of the 2010 European Rotorcraft Forum, September 2010.

[28] Rajmohan, N., Bain, J, Nucci, M., Sankar, L., Flemming, R. J., Egolf, A., Kreeger, R., "Icing Studies for the UH-60A Rotor in Forward Flight," Proceedings of AHS Aeromechanics Specialists' Conference, Jan 20-22, 2010.

[29] Bain, J., Sankar, L. N.,Deresz, R., Egolf, T. A., Flemming, R. J., and Kreeger, R., "Effects of Icing on Rotary Wing Loads and Surface Heat Transfer Rates," AIAA2011-1100, 49th AIAA Aerospace Sciences Meeting including the New Horizons Forum and Aerospace Exposition, Orlando, Florida, Jan. 4-7, 2011.

[30] Bain, J., Sankar, L. N., Garza, D., Aubert, R. J., and Flemming, R. J., "A Methodology for the Prediction of Rotor Blade Ice Formation and Shedding," Proceedings of the SAE 2011 Aircraft and Engine icing and Ground Testing Conference, June 13-17, 2011.

[30] Narducci, R. and Kreeger, R., "Analysis of a Hovering Rotor in Icing Conditions," Proceedings of American Helicopter Society 66th Annual Forum, 2010.

[32] Narducci, R., Orr, S. and Kreeger, R., "Application of a High-Fidelity Icing Analysis Method to a Model-Scale Rotor in Forward Flight," Proceedings of American Helicopter Society 67th Annual Forum, 2011.

[33] Kim, Jeewoong, "Development of a Physics Based Methodology for the Prediction of Rotor Blade Ice Formation," PhD Dissertation, Georgia Institute of Technology, Atlanta, GA, December 2015.

[34] Soltis, J., Palacios, J., Eden, T., Douglas, W., "Evaluation of Ice-Adhesion Strength on Erosion-Resistant Materials," AIAA Journal Vol. 53-7, July 2015,

[35] Tarquini, S., Antonini, C., Amirfazli, A., Marengo M., Palacios, J., "Investigation of ice shedding properties of superhydrophobic coatings on helicopter blades," Cold Regions Science and Technology, 100 (2014) 50-58.

APPPENDIX A

Table A.1. Summary of Shedding Calculations

Case	Temperature (°C)	MVD (µm)	LWC (g/m^3)	RPM	Collective (°)	Experimental Shedding Location	Predicted Shedding Location	Total Icing Time (s)
1	-10.7	25	2.0	600	2.5	-	No Shedding	180
2	-4.7	20	6.9	600	2.5	0.77 R	0.80 R	352
3	-5	30	2.0	450	2.5	Not Available	0.65 R	352
4	-10	30	2.0	450	2.5	Not Available	No Shedding	352
5	-15	30	2.0	450	2.5	Not Available	No Shedding	352
6	-5	30	0.5	450	2.5	Not Available	No Shedding	352
7	-5	30	5.0	450	2.5	Not Available	0.55 R	352
8	-5	20	2.0	450	2.5	Not Available	0.45 R	352
9	-5	40	2.0	450	2.5	Not Available	0.75 R	352